

Research Report

Evaluation of a Novel Cystoscopic Compatible Cryocatheter for the Treatment of Bladder Cancer

John M. Baust^{a,*}, Anthony Robilotto^a, Kimberly L. Santucci^a, Kristi K. Snyder^a, Robert G. Van Buskirk^{a,b,c}, Aaron Katz^d, Anthony Corcoran^d and John G. Baust^{b,c}

^a*CPSI Biotech, Owego, NY, USA*

^b*Center for Translational Stem Cell and Tissue Engineering Binghamton University, Binghamton, NY, USA*

^c*Department of Biological Sciences, Binghamton University, Binghamton, NY, USA*

^d*Department of Urology, NYU Winthrop Hospital, Mineola, NY, USA*

Received 29 April 2020

Accepted 3 July 2020

Pre-press 6 August 2020

Published 21 September 2020

Abstract.

BACKGROUND: As the acceptance of cryoablative therapies for the treatment of non-metastatic cancers continues to grow, avenues for novel cryosurgical technologies and approaches have opened. Within the field of genitourinary tumors, cryosurgical treatments of bladder cancers remain largely investigational. Current modalities employ percutaneous needles or transurethral cryoballoons or sprays, and while results have been promising, each technology is limited to specific types and stages of cancers.

OBJECTIVE: This study evaluated a new, self-contained transurethral cryocatheter, *FrostBite-BC*, for its potential to treat bladder cancer.

METHODS: Thermal characteristics and ablative capacity were assessed using calorimetry, isothermal analyses, *in vitro* 3-dimensional tissue engineered models (TEMs), and a pilot *in vivo* porcine study.

RESULTS: Isotherm assessment revealed surface temperatures below -20°C within 9 sec. *In vitro* TEMs studies demonstrated attainment of $\leq -20^{\circ}\text{C}$ at 6.1 mm and 8.2 mm in diameter following single and double 2 min freezes, respectively. Fluorescent imaging 24 hr post-thaw revealed uniform, ablative volumes of 326.2 mm^3 and 397.9 mm^3 following a single or double 2 min freeze. *In vivo* results demonstrated the consistent generation of ablative areas. Lesion depth was found to correlate with freeze time wherein 15 sec freezes resulted in ablation confined to the sub-mucosa and ≥ 30 sec full thickness ablation of the bladder wall.

CONCLUSIONS: These studies demonstrate the potential of the *FrostBite-BC* cryocatheter as a treatment option for bladder cancer. Although preliminary, the outcomes of these studies were encouraging, and support the continued investigation into the potential of the *FrostBite-BC* cryocatheter as a next generation, minimally invasive cryoablative technology.

Keywords: Cryoablation, FrostBite, PSN, cryoprobe, tissue engineered models, porcine model, bladder cancer

INTRODUCTION

As medical technologies and treatment modalities continue to advance, there is growing desire among patients and physicians for more minimally invasive treatment options for non-metastatic, cancerous

*Correspondence to: John M. Baust, Ph.D., CPSI Biotech, 2 Court St. Owego, NY 13827, USA. Tel.: +1 (607) 687 8701; E-mail: jmbaust@cpsibiotech.com.

lesions. To this end, the use of cryotherapy has been shown to be an effective primary treatment option in a number of cancers and has seen rapid growth in recent years [1–3]. Cryotherapy offers several benefits over other treatments including hyperthermic (heat-based) ablative approaches. Cryotherapy has been shown to have shorter procedure times, is safe, produces less pain and operator stress, and has fewer unintended side-effects [4–10]. Cryolesion formation can be visualized using ultrasound whereas hyperthermic ablation lesions cannot. Importantly, cryolesions do not “grow” post treatment whereas heat-based lesions will increase in size (depth) for several days, clinically resulting in a higher risk of complications [11–14]. Other benefits include depth of penetration, ability to use in combination with other treatments (adjunctive role), likely improved hemostasis and the ability to target non-resectable tumors [15–18]. Through percutaneous needles or catheter-based approaches, the delivery of cryoablative doses to tissues not traditionally targeted by the therapy have expanded [19–29]. Yet for such therapies to be clinically viable, the cryotherapeutic approach must be able to deliver ablative temperatures in a confined, controlled, and time efficient manner. Furthermore, the development and evaluation of these novel platforms and approaches must be done in such a way as to streamline the transition from laboratory prototypes to commercially available technologies.

One such area of interest is in the treatment of bladder cancers (BC). Though less common in females, BC is the fourth most common cancer among men and has the highest lifetime cost of all cancers [30, 31]. Current treatment options depend largely on the stage and grade of the cancer. For superficial (stage 0is), non-invasive (stage 0a), and non-muscle invasive (stage 1) BCs, treatment is most commonly transurethral resection (TUR) followed by intravesical therapy with chemotherapeutic or immunotherapeutic agents. For more advanced, muscle invasive lesions (stages 2–4), partial or radical cystectomy, radiation, and/or systemic chemotherapy are performed. The use of cryotherapy as a minimally invasive primary, or combinatorial, treatment option for BC has previously been reported [32–41], and while the results have been promising, its use remains largely investigational.

In this study we assessed a new cystoscopic compatible cryocatheter (*FrostBite-BC*) in conjunction with the Pressurized Sub-cooled Nitrogen (PSN) cryoconsole for the cryoablation of BC. Using a

mixed phase liquid (LN_2) and gaseous (N_2) nitrogen cryogen, the PSN device is able to rapidly deliver sub-lethal temperatures through a number of cryoprobe configurations and serves as a versatile cryoconsole platform for ablating various tissues and organ systems. In this study, PSN in conjunction with the prototype transurethral cystoscopic compatible cryocatheter, *FrostBite-BC*, the ability to deliver rapid and effective ablative doses for the treatment of BC was assessed. Through the use of acellular hydrogels; *in vitro*, 3-dimensional tissue engineered models (TEMs); and a pilot, *in vivo* porcine study, we set out to characterize and evaluate the *FrostBite-BC* cryocatheter and demonstrate its potential as a treatment option for a range of BC types and stages including Stage 1–3 BC (non-muscle invasive and muscle invasive BC).

METHODS

Pressurized sub-cooled nitrogen (PSN) system and bladder cryoprobe

All tests were performed using the PSN cryosurgical device (CPSI Biotech, Owego, NY) with an input N_2 pressure of 1,500 psi. The *FrostBite-BC* cryoablation catheters (CPSI Biotech) employed in these studies were a 6.5 Fr (2.18 mm OD) \times 44.5 cm long and an 8 Fr (2.70 mm OD) \times 44.5 cm long flexible catheters. Both catheters had a 14 gauge (2.1 mm diameter \times 7.5 mm length) stainless steel, blunt tip ablation segment and were connected to the PSN console by a 300 cm umbilical.

Isotherm and calorimetry testing

Isotherm testing

The distal end of the 6.5 Fr bladder cryocatheter was inserted into an isotherm test fixture consisting of an acrylic box filled with $20^\circ\text{C} \pm 2^\circ\text{C}$ ultrasound gel and a thermocouple mandrel affixed with 5, 36 Ga type-T thermocouples. The midpoint of the cryocatheter freeze segment was positioned on the mandrel such that the thermocouples were positioned at 0, 2.5, 5.0, 7.5, and 10.0 mm extending radially from the cryocatheter surface (Fig. 1A). With the cryoprobe centered in the test fixture, a 2 min freeze procedure was performed with temperatures recorded at a rate of 1/sec using an Omega OMB-DaqScan 2000 Series device (Omega Engineering, Norwalk, CT).

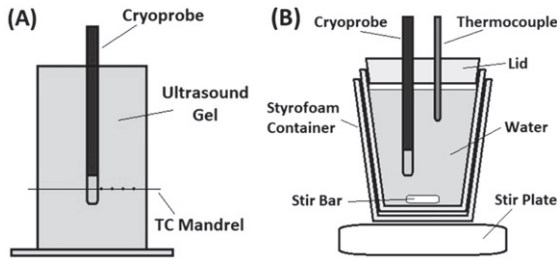


Fig. 1. Illustrations of the Isothermal and Calorimetry Testing Fixtures. The isothermal test fixture (A) consisted of an acrylic box filled with $20^{\circ}\text{C} \pm 2^{\circ}\text{C}$ ultrasound gel and a mandrel with 5, type-T thermocouples at distances of 0, 2.5, 5.0, 7.5, and 10.0 mm extending radially from the cryocatheter surface. Temperature recordings, taken at a rate of 1/sec, were used to determine the distribution of critical isotherms within the iceball generated during a 2 min freeze. The calorimetry vessel (B) consisted of a styrofoam container filled with 454 mL of $32^{\circ}\text{C} \pm 1^{\circ}\text{C}$ water placed on a magnetic stir plate. A type-T thermocouple needle was used to monitor the temperature drop over a 2 min freeze procedure and the data was used to calculate the cooling power of the cryocatheter.

Calorimetry testing

Calorimetry testing was conducted using a 30 mm t-style magnetic stir-bar placed into the bottom of a 20 oz double walled foam insulated vessel. The insulated vessel was filled with 454 mL of $32^{\circ}\text{C} \pm 1^{\circ}\text{C}$ water and a ~ 20 mm thick polystyrene lid was placed on top. The setup was placed on a magnetic stir plate and the speed was set to the highest setting in which the stir-bar maintained uniform spinning (setting 8 out of 11). The cryoprobe ablation zone was placed through a tight fitting hole in the lid with the distal end 20 mm from the bottom of the vessel (to ensure that the entire freeze zone was submerged but did not contact the stir bar or the vessel wall). A 21 ga (0.032 inch) type-T thermocouple needle was inserted through the lid into the water to monitor the temperature change (Fig. 1B). A 2 min freeze procedure was performed and the starting and ending water temperatures were recorded.

Cooling power was determined using standard calorimetry calculations.

$$P = \frac{\Delta Q}{\Delta t} = \frac{m_w \cdot s_w \cdot \Delta T}{\Delta t}$$

Where P =cooling power, Q =heat energy, m_w =mass of water, s_w =specific heat of water ($4.186 \text{ J/g}^{\circ}\text{C}$), T =temperature, and t =time (length of freeze procedure).

Cell and 3D TEM culture

Cell cultures were maintained in T-75 CellTreat flasks (CellTreat, Shirley, MA) in 95% $\text{O}_2/5\%$ CO_2 incubators and passaged at 80–85% confluence with media replenishment every three days. SCaBER cells and UMUC3 BC cells (ATCC, Rockville, MD) were cultured in Eagle's Minimum Essential Medium (ATCC #30-2003) with 10% FBS (Peak Serum, #PS-FB3, Wellington, CO) and 1% penicillin/streptomycin (Lonza, #17-602E, Walkersville, MD). All experiments were performed between cell passages 5 and 20. SCaBER cells are a human urinary bladder squamous cell carcinoma and UMUC3 cells are a human urothelial carcinoma (urinary bladder transitional cell carcinoma). Cell Identity: Both cell lines used in this study were purchased directly from ATCC. Neither cell line is listed in the database of commonly misidentified cell lines maintained by the International Cell Line Authentication Committee (Version 10, March 25, 2020).

For generation of the tissue engineered models (TEM), rat tail type I collagen solution (BD Bioscience, Bedford, MA) was used to form 0.2% w/v gel matrices as per SOP. Cells (1.5×10^6 cells/mL) were suspended in the collagen solution prior to solidification in 40×48 mm TEM ring fixtures and then placed in 100 mm petri dishes, and allowed to solidify for 30 min in a 37°C hybridization oven as per Robilotto et al. and Baust et al. (42–45). Following gelation, 15 mL of cell culture medium was added to the dish to cover the TEMs and the dishes were placed in the incubator. The TEM cell containing matrices were cultured for 24 hours prior to utilization.

Freeze procedure

All tests were performed in a laminar flow hood to ensure sample sterility (Fig. 2). Briefly, an acrylic box with a suspended mesh platform was filled with Milli-Q grade water warmed to 37°C and placed into a water bath maintained at $35^{\circ}\text{C} \pm 2^{\circ}\text{C}$. The *FrostBite* cryocatheter was inserted into the test fixture consisting of a Pentax ES-3870K endoscope (Pentax, Tokyo, Japan) submerged in the 35°C bath to simulate heat load on the catheter and ablation tip during a procedure. The cryocatheter was extended ~ 10 cm out the distal end of the endoscope, inserted through a sealable opening on the bottom of the acrylic box, and placed perpendicular to the suspended mesh platform. The 10 cm extension length was utilized to properly position the ablation segment against the

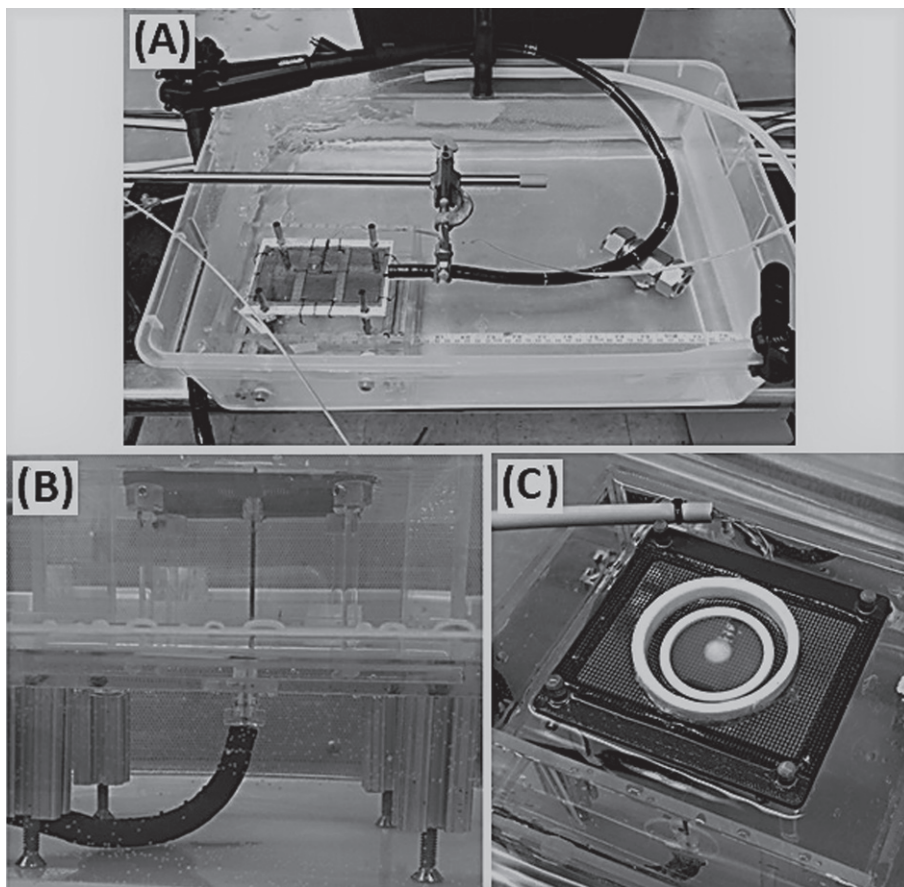


Fig. 2. Images of the *In Vitro* TEM Freeze Experimental Setup. The test set up consisted of an endoscope and an acrylic box containing the TEM platform submerged in a 37°C water bath (A). The cryocatheter was inserted through the scope and the distal end was passed through a sealable gasket on the bottom of the TEM box and placed perpendicular to a mesh platform holding the TEM (B). The SCaBER and UMUC3-TEMs were then placed on the mesh platform, centered over the cryocatheter, and the acrylic box was filled with 37°C Milli-Q grade water to a level even with the TEM ring/probe interface (C).

tissue within the fixture. The TEM ring was then placed on top of the mesh platform and centered over the cryocatheter tip. Freezing was either a single 2 min freeze or a repeat 2/2/2 min freeze/thaw/freeze double freeze procedure. Temperatures of the transmural surface of the TEMs (the side opposite the cryocatheter) were monitored using a FLIR T650sc IR camera (FLIR Systems Inc., Wilsonville, OR). IR photos of the transmural surface were taken following the single and repeat 2 min freezes and analyzed using FLIR ResearchIR Max software (FLIR Systems Inc.). Following freezing, the TEMs were allowed to thaw passively for 5 min then returned to culture.

Cell viability assessment

Following thawing, individual TEMs were measured via calipers to determine the diameter of the

iceball created following the 1st and 2nd freezes of the freeze-thaw cycle. Iceball radii were measured at cardinal locations around the probe surface to determine symmetry of the freeze zone created. TEMs were then placed into culture to assess at 24 hrs and 72 hrs post-freezing recovery. *In situ* sample viability assessment (live/dead assay) was performed using the fluorescent probes Calcein-AM and Propidium Iodide (Cal/PI; Molecular Probes, Eugene, OR). Briefly, culture medium was decanted from the TEM samples and a working solution of 5 µg/mL Calcein-AM (live cells) and 4 µg/mL propidium iodide (necrotic cells) in 1X PBS (Corning) was added directly to each sample. Samples were incubated in the dark at 37°C for 60 min (± 1 min). Fluorescent staining was visualized using a Zeiss Axio Observer 7 with ZEN software (Carl Zeiss AG, Oberkochen, Germany). Panoramic digital images spanning the center of the freeze zone

were stitched together from a 6×30 set of overlapping images using a 10X objective. Following acquisition, a 2 mm scale bar was imprinted onto each of the images to enable direct image comparison. Diameters of the necrotic zones were then measured using the ZEN software measurement tool.

Pilot in vivo porcine study

In vivo testing was performed in a porcine model at American Preclinical Services (Coon Rapids, MN) under IACUC approval (IACUC approval number 19-0792). Two animals with 7 day survival were enrolled in the study. Each animal had two laparoscopic trocars placed through the lower abdomen near the urinary bladder; one on the left side of midline and the other on the right side. A custom-built surface thermocouple was placed on the outside of the bladder wall through one of the laparoscopic ports where possible, while the other port was used to insert a laparoscopic camera to visualize ice formation on the outer wall of the bladder where possible. A 21Fr Olympus cystoscope (A20911A) with an Olympus lens (A2011A) was used to access and visualize the bladder through the urethra, the *FrostBite-BC* catheter was inserted through the cystoscope using a Olympus bridge (A2976), the ablation tip advanced 2 to 3 cm beyond the end of the cystoscope, and placed against the inner wall of the bladder. Once the ablation tip was in position and visualized with both cystoscopic and laparoscopic cameras, the freeze procedure was initiated. Observations of probe tip temperature, time to visual ice on the inner and outer wall of the bladder, outer wall temperature, freeze time, and lesion location were recorded. Each animal had 12 ablations performed within the bladder for durations of 15 sec, 30 sec, 60 sec, or 90 sec. Animals were allowed to recover after the procedure and were maintained (survived) for approximately seven days prior to euthanasia. Necropsy evaluations and imaging of observed pathological changes were performed for both animals. The urinary bladders were removed and fixed unopened with luminal installation of 10% NBF. After fixation was complete, the bladder mucosa was exposed and imaged prior to treatment site sampling for histopathology. Representative samples trimmed from the tissues were processed routinely for paraffin embedding and stained with hematoxylin and eosin (H & E) for light microscopy histopathology evaluation. Qualitative assessments were performed to assess transmural of each urinary bladder lesion.

Table 1
Isotherm Diameters (\pm SD) for the FrostBite-BC Cryocatheter Following a 2 min Freeze in a 20°C Acellular Hydrogel

Isotherm Diameter (mm \pm (SD))				
0°C	-10°C	-20°C	-30°C	-40°C
16.7 (0.70)	9.8 (0.83)	8.5 (0.78)	5.7 (0.62)	5.2 (0.79)

Data analysis

All *in vitro* tests had a minimum of 3 repeats. Following testing, data were combined and averaged (\pm standard deviation) to determine mean iceball size, isotherm distribution, cooling power, and ablative diameter. Statistical significance was determined using single factor ANOVA where noted.

RESULTS

Isotherm distribution

To characterize the performance of the cryocatheter a series of studies were conducted to assess the isotherm distribution around the ablation segment. A 2 min freeze duration was selected based on previous reports suggesting that the PSN system rapidly delivers ablation temperatures and as such extended freeze times are unnecessary [18]. Following a single 2 min freeze in 20°C \pm 2°C ultrasound gel, the 6.5 Fr blunt tip bladder cryocatheter created an iceball 16.7 mm (\pm 0.7) in diameter (Table 1). The overall size of the iceball, however, is not predictive of the distribution of isotherms within the frozen mass. A more clinically relevant metric is to determine the extent of the spread of critical isotherms or minimal lethal temperature, the temperature below which complete cell destruction occurs in the targeted tissue. Previous *in vitro* studies have reported a minimal lethal temperature for SCaBER and UMUC3 cells of -25°C following a single 5 min freeze exposure and -20°C for double 5 min freeze exposure [46]. This and other reports have also demonstrated that attainment of the minimal lethal temperature for \geq 30 sec to achieve cell death [44, 46, 47]. As such shorter freeze intervals are possible if target temperatures are attained. To determine the temperature distributions within the frozen mass generated by the *FrostBite-BC* cryocatheter, an array of thermocouples was utilized in the test setup. Examining these results revealed diameters of 8.5 mm (\pm 0.8) for the -20°C isotherm and 5.7 mm (\pm 0.6) for the -30°C isotherm following a single 2 min freeze procedure, indicating a clinically destructive ablation volume of >321.6 mm³.

Table 2
Calorimetry Data (\pm SD) for the FrostBite-BC Cryocatheter Following a 2 min Freeze

Water Temperature ($^{\circ}$ C \pm (SD))			Cooling Power (W \pm (SD))
Start	End	Δ T	
32.6 (0.06)	30.7 (0.06)	1.9 (0.10)	30.1 (1.58)

Calorimetry testing

While less common with cryoablation devices, ablation segment power (wattage) is often used to compare hyperthermal (heat-based) device efficacy. As such we conducted a series of calorimetry studies to characterize the heat extraction (ablation) power of the cryocatheter. For cooling power evaluations of the prototype, *FrostBite* cryocatheter, a starting water temperature of 32° C \pm 1° C was used. This temperature was selected due to previous testing (not shown) that showed ice formation at these temperatures in the calorimetry vessel to be minimal (<1 mm diameter) [44, 48]. At warmer temperatures, no ice was observed indicating inefficient flow (complete boiling) of the cryogen. At colder temperatures, however, ice began to accumulate along the freeze segment of the probe insulating the freeze surface from the surrounding water. At the ideal water temperature of 32° C \pm 1° C, calorimetric analysis was conducted (Table 2). Results showed an average decrease in water temperature of 1.9° C (\pm 0.1) following 2 min of freezing. This calculated to a cooling power of 30.1 W (\pm 1.6), or 0.57 W/mm² of surface area.

Freezing of tissue engineered models (TEMs)

While the use of acellular hydrogels and calorimetric testing can provide relevant data on the generation and spread of critical isotherms and the cooling power of cryoprobes, such testing does not provide information on the response of cells or tissues to the freezing regime. To that end, employing *in vitro*, 3-dimensional tissue constructs in the clinically analogous test setup provided a means by which the thermal performance of the bladder cryocatheter, as well as cellular responses, may be assessed. These TEMs enable accelerated R & D and allow for follow up recovery studies to assess the impact of delayed tissue damage. This robust model has been shown to provide vital information on *in vivo* response while reducing the expense and burden of exploratory animal studies [42–44, 49]. Two BC cell lines were chosen for these studies: SCaBER cell, a squamous

cell carcinoma representing an aggressive basal, muscle invasive BC, and UMUC3 cells, a transitional cell carcinoma representing an intermediate to high risk BC.

Transmural surface temperatures

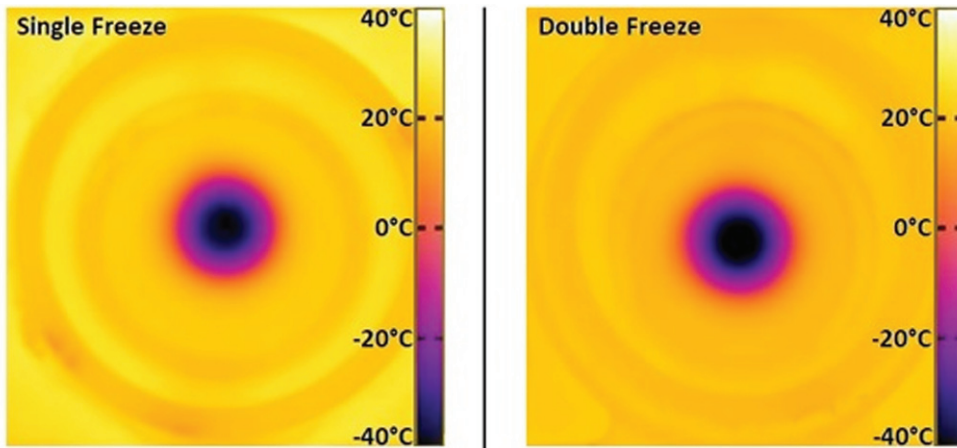
Successful ablation of muscle invasive BCs requires the generation of lethal temperatures through the full thickness of the bladder wall. By monitoring the transmural surface of the TEMs with an IR camera, the propagation of these isotherms could be monitored in real time. For the SCaBER-TEMs (Fig. 3A), following a single 2 min freeze the transmural surface had a frozen diameter of 12.5 mm (\pm 0.8) which grew to 13.4 mm (\pm 2.0) following 2 min of thawing and a repeat 2 min freeze. This equates to an area of 122.7 mm² for a single freeze and 141.0 mm² for a double freeze. Within this frozen area, the -20° C and -30° C critical isotherms had diameters of 6.2 mm (\pm 3.1) (area 30.2 mm²) and 2.7 mm (\pm 2.1) (area 5.7 mm²) respectively following a single freeze, and 7.7 mm (\pm 2.6) (area 46.6 mm²) and 4.1 mm (\pm 3.4) (area 13.2 mm²) following a repeat freeze.

The UMUC3-TEMs had similar transmural temperatures (Fig. 3B). Following a single 2 min freeze, the 0° C, -20° C, and -30° C isotherms had diameters of 12.0 mm (\pm 1.6), 6.0 mm (\pm 3.1), and 2.8 mm (\pm 2.2) respectively, which equated to areas of 113.1 mm², 28.3 mm², and 6.2 mm². At the end of the 2/2/2 min freeze/thaw/freeze procedure, the iceball had a diameter of 14.1 mm (\pm 1.6) (area 156.1 mm²), the -20° C isotherm had a diameter of 8.7 mm (\pm 1.6) (area 59.4 mm²), and the -30° C isotherm had a diameter of 5.2 mm (\pm 1.7) (area 21.2 mm²). Taking the SCaBER and UMUC3 data together, iceball diameters increased an average of 1.5 mm between a single and double 2 min freeze. Isothermal analysis revealed that the -20° C and -30° C isotherm increased to a greater extent compared with the iceball, an average increase of 2.1 mm and 1.9 mm, respectively.

TEM viability

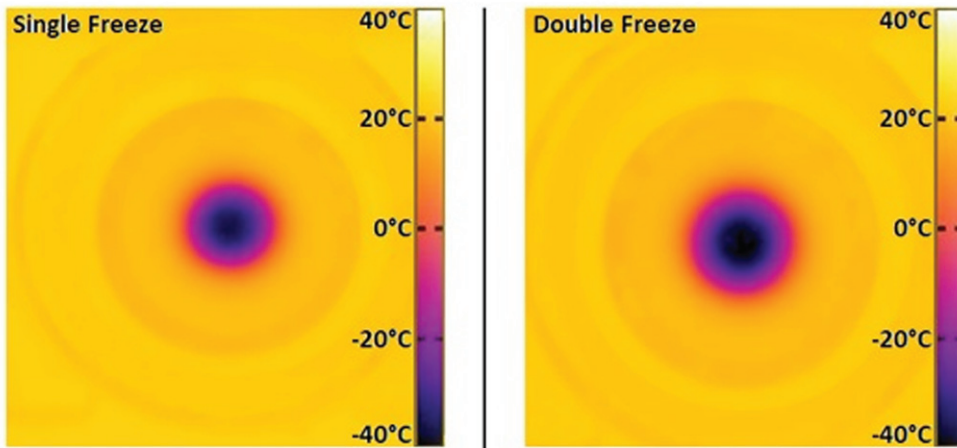
In addition to the size and isotherm distribution of the freeze zones generated with the prototype *FrostBite-BC* cryocatheter, the ablative zones created in the TEMs were also assessed using fluorescent microscopy post-thaw. TEMs frozen with a single 2 min and repeat 2/2/2 min procedure were stained with Calcein-AM (green, live) and Propidium Iodide (red, necrotic) at 24 hr and 72 hr post-thaw to determine the extent of cell death within the frozen volume

(A) SCaBER-TEM



	Single 2 min Freeze					Double 2 min Freeze					Dia (mm)
	0°C	-10°C	-20°C	-30°C	-40°C	0°C	-10°C	-20°C	-30°C	-40°C	
Dia (mm)	12.5 (0.76)	9.4 (1.54)	6.2 (3.12)	2.7 (2.14)	0.2 (0.45)	13.4 (1.98)	10.4 (2.37)	7.7 (2.55)	4.1 (3.37)	0.9 (2.20)	Dia (mm)
Area (mm²)	123.1 (14.71)	71.3 (20.92)	36.2 (19.77)	8.9 (11.13)	0.2 (0.39)	143.9 (39.85)	89.2 (35.39)	50.6 (27.86)	20.9 (19.43)	3.8 (9.35)	Area (mm²)

(B) UMUC3-TEM



	Single 2 min Freeze					Double 2 min Freeze					Dia (mm)
	0°C	-10°C	-20°C	-30°C	-40°C	0°C	-10°C	-20°C	-30°C	-40°C	
Dia (mm)	12.0 (1.56)	9.3 (1.70)	6.0 (3.05)	2.8 (2.16)	0.0	14.1 (1.59)	11.2 (1.65)	8.7 (1.55)	5.2 (1.73)	0.7 (1.63)	Dia (mm)
Area (mm²)	114.1 (29.28)	69.3 (23.74)	34.1 (21.35)	9.1 (7.31)	0.0	157.1 (36.50)	100.6 (29.72)	60.8 (21.46)	23.1 (14.41)	2.1 (5.13)	Area (mm²)

Fig. 3. IR Images of the Transmural Surface of the TEMs Following Single and Double 2 min Freezes. During TEM freeze testing the transmural surface (the side opposite the cryocatheter) of the SCaBER-TEMs (A) and UMUC3-TEMs (B) were imaged with an IR camera. The TEM rings, being of known diameter, were used to calibrate measurements of isotherm diameters presented in the tables below the images. The combined average diameters of the 0°C, -20°C, and -30°C isotherms were 12.2 mm, 6.1 mm, and 2.8 mm respectively following a single 2 min freeze and 13.7 mm, 8.2 mm, and 4.7 mm following a repeat freeze.

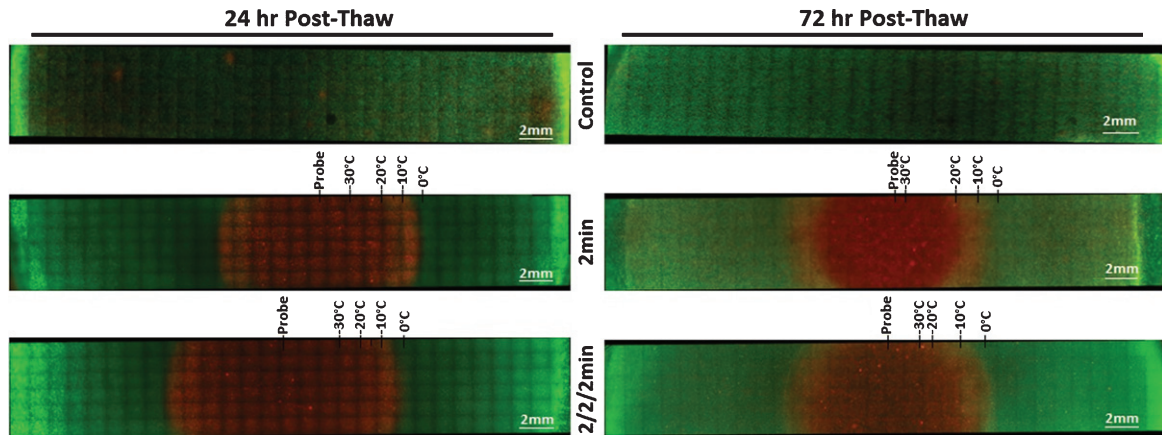


Fig. 4. Fluorescent Micrographs of the SCaBER-TEMs Following Single and Double 2 min Freezes. At 24 hr (A) and 72 hr (B) post-thaw, unfrozen controls, single freeze, and double freeze TEMs were probed with Calcein-AM (green, live) and Propidium Iodide (red, dead) and visualized using fluorescent microscopy to determine the extent of cell death. Images were stitched together from a 6×30 set of overlapping images using a 10X objective. Measurements were made using the Zeiss ZEN software and temperatures from the corresponding IR images were mapped to the micrographs.

Table 3

Diameters and Areas (\pm SD) of Frozen and Ablative Zones for SCaBER and UMUC3-TEMs at 24 hr and 72 hr Following Single and Double 2 min Freezes

		24 hr Post-Thaw				72 hr Post-Thaw			
		Single 2 min		Double 2 min		Single 2 min		Double 2 min	
		Freeze Zone	Necrotic Zone	Freeze Zone	Necrotic Zone	Freeze Zone	Necrotic Zone	Freeze Zone	Necrotic Zone
SCaBER-TEMs	Dia. (mm \pm (SD))	12.8 (1.15)	12.2 (0.55)	14.3 (0.30)	13.8 (0.50)	12.3 (0.68)	9.6 (1.22)	13.0 (1.95)	10.4 (2.24)
	Area (mm ² \pm (SD))	128.7 (23.03)	117.7 (10.45)	160.7 (6.74)	149.0 (10.92)	118.4 (12.95)	73.2 (19.00)	134.7 (40.12)	87.0 (37.65)
	Volume (mm ³ \pm (SD))	386.1 (3.68)	350.7 (0.64)	481.8 (0.21)	448.7 (0.6)	356.5 (1.09)	217.2 (3.51)	398.2 (8.69)	254.9 (11.8)
UMUC3-TEMs	Dia. (mm \pm (SD))	12.5 (0.84)	11.3 (1.47)	13.0 (1.12)	12.6 (0.51)	12.0 (1.65)	8.9 (2.33)	14.6 (1.40)	12.3 (0.32)
	Area (mm ² \pm (SD))	122.4 (16.11)	101.4 (26.66)	132.7 (23.23)	124.2 (10.05)	114.5 (29.81)	65.1 (30.88)	167.7 (32.18)	119.5 (6.27)
	Volume (mm ³ \pm (SD))	368.2 (1.66)	300.9 (5.1)	398 (2.86)	374.1 (0.61)	339.3 (1.09)	186.6 (12.46)	502.3 (4.62)	356.5 (0.24)

(Figs. 4 (SCaBER) and 5 (UMUC3)). As Calcein-AM and Propidium Iodide are single end-point assessments, sister samples were used to assess viability following 24 hr and 72 hr of recovery. For both cancer cell types, non-frozen control TEMs showed no cell death over the course of the 72 hr incubation period. Measurements of the iceball diameter and the extent of cell death in frozen/thawed TEMs were made using the ZEN software and results, averaged from triplicate experiments (Table 3).

The average size of the frozen areas measured on the micrographs corresponded to within 1 mm of those obtained with the transmural IR data. The freeze diameter was 12.4 mm (386.1 mm³) for all single 2 min freezes and 13.7 mm (481 mm³) for double

2 min freezes (SCaBER and UMUC3 data averaged). Following 24 hr of recovery, the SCaBER-TEMs had a zone of necrosis 12.2 mm (\pm 0.6) in diameter (350.7 mm³) after a single freeze and a 13.8 mm (\pm 0.5) diameter (area 448.7 mm³) after a double freeze. After 72 hr of recovery, the necrotic diameter decreased to 9.6 mm (\pm 1.2) (217.2 mm³) and 10.4 mm (\pm 2.2) (259.9 mm³) for the single and double 2 min freezes, respectively. A reduction in the size of the ablative zone between 24 hrs and 72 hrs post-thaw was also observed in the UMUC3-TEMs (Fig. 5, Table 3). For a single 2 min freeze, the necrotic diameter decreased from 11.3 mm (\pm 1.5) (area 300.9 mm³) to 8.9 mm (\pm 2.3) (186.6 mm³) and from 12.6 mm (\pm 0.5) (374.1 mm³) to 12.3 mm (\pm 0.3) (356.5 mm³)

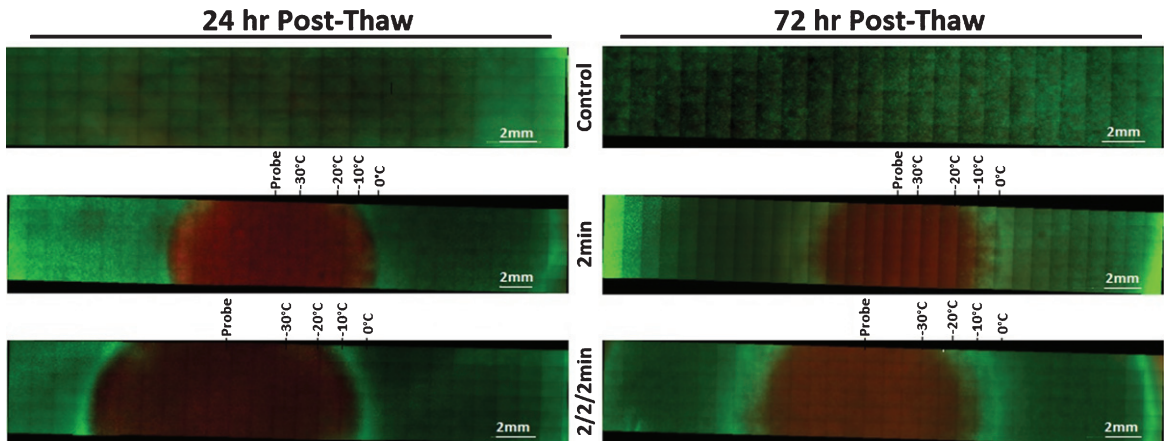


Fig. 5. Fluorescent Micrographs of the UMUC3-TEMs Following Single and Double 2 min Freezes. At 24 hr (A) and 72 hr (B) post-thaw unfrozen controls, single freeze, and double freeze TEMs were probed with Calcein-AM (green, live) and Propidium Iodide (red, dead) and visualized using fluorescent microscopy to determine the extent of cell death. Images were stitched together from a 6×30 set of overlapping images using a 10X objective. Measurements were made using the Zeiss ZEN software and temperatures from the corresponding IR images were mapped to the micrographs.

for the dual 2 min freeze procedure. Previous studies have shown that this reduction is attributed to a combination of cellular recovery, infiltration and regrowth in the periphery of the cryogenic lesion over the 3 day recovery period in the region where temperatures are above the minimal critical temperature [42, 43, 49, 50].

In vivo porcine study

In addition to *in vitro* assessment of *FrostBite-BC* cryocatheter performance, a pilot *in vivo* porcine animal study was also conducted. The study consisted of two female pigs with up to 12 lesions created in each bladder. An 8 Fr *FrostBite-BC* cryocatheter was inserted through a 21 Fr cystoscope, extended beyond the distal end of the scope, and placed along the mucosal surface of the bladder. Visualization of the freeze was achieved via the cystoscope and a laparoscopic camera inserted through a trocar placed in the lower abdomen near the bladder. The initial freeze was set at 2 min in order to assess the correlation between TEM data and the *in vivo* procedures. However, the initial lesion was stopped following 90 sec of freezing as ice formation was observed on the inner and outer bladder wall within 15 sec. Following 90 sec of freezing, an outer wall temperature of -30°C and probe tip temperature of -120°C was recorded. The improved performance observed *in vivo* was likely due to increased cryocatheter ablation tip/tissue contact area and increased pressure of the catheter tip on the bladder wall compared to that

used in the TEM studies. For subsequent ablations, freeze times of 15 sec, 30 sec, 60 sec, and 90 sec were performed.

A set of time lapse, cystoscopic images taken during a 30 sec freeze are shown in Fig. 6A. Ice formation along the mucosal surface of the bladder was observed by $12 (\pm 2)$ sec, and ice continued to grow over the course of the 30 sec ablation. Using laparoscopic visualization and thermocouple placement, ice formation on the outer wall (freeze through) was noted within 10 sec. Temperature monitoring revealed that the cryocatheter tip achieved sub-freezing temperatures within 3 sec of the initiation of cryogen flow, and at the conclusion of the 30 sec freeze the surface had attained a nadir temperature of $-96^{\circ}\text{C} (\pm 4)$ (Fig. 6B). For the 60 sec freeze procedures, initial ice formation on the inner and outer wall of the bladder was observed at 14 sec (± 2) and 8 sec (± 2), respectively. Temperatures at the probe surface were $-95^{\circ}\text{C} (\pm 5)$ and $-15^{\circ}\text{C} (\pm 3)$ on the outer wall surface ~ 5 mm from the probe tip following a 60 sec freeze. For all freeze procedures, on average the cryocatheter tip was found to passively thaw and release from the bladder wall within ~ 1 min (50 sec (± 15 sec)) of cessation of cryogen flow. Importantly, regardless of the freeze time it was noted that upon cessation of the freeze procedure, the surface temperature immediately began to warm, thus preventing any carryover damage to the bladder wall or adjacent tissues.

Following the *in vivo* freeze procedures, animals were survived for 7 days prior to euthanasia.

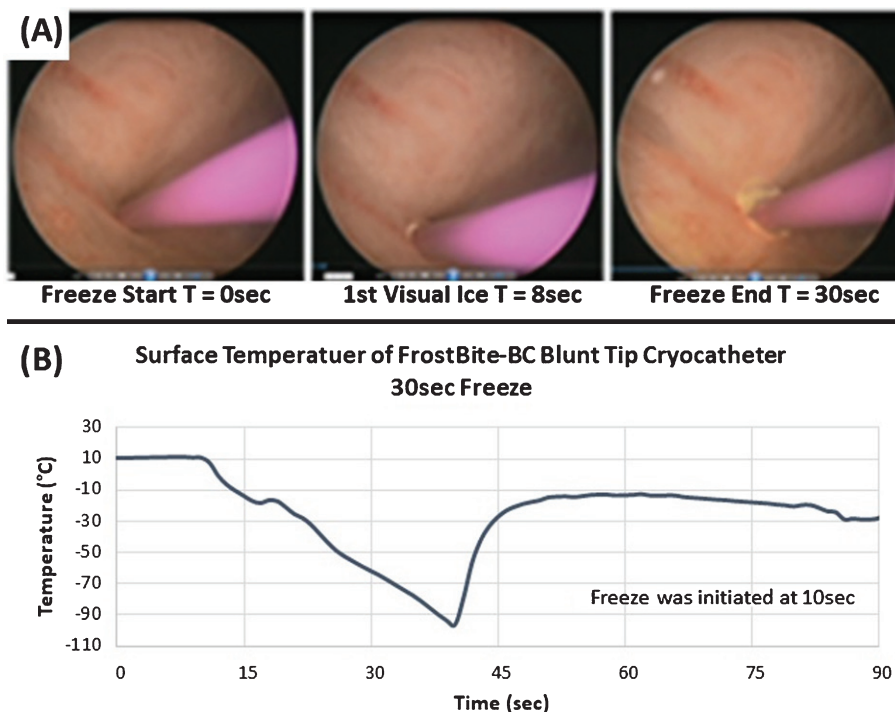


Fig. 6. Time Lapse Cystoscopic Images and Thermal Profile of an *In Vivo* Porcine Freeze Procedure. Images (A) illustrate the application of a 30 sec freeze in the bladder performed via transurethral introduction with cystoscopy guidance. Images depict probe positioning (T = 0 sec), initial visual ice (T = 8 sec), and the final frozen tissue mass (T = 30 sec). Temperature monitoring of the probe tip surface (B) revealed a nadir temperature of -96.4°C and the resulting lesion created an ablated area of bladder wall tissue ~ 12 mm in diameter.

The bladders were then resected and fixed, and both gross pathological and histological analyses were performed. The dorsal and ventral serosal surfaces of one of the bladders is shown in Fig. 7A and B, with the green inked sites indicating the presence and location of transmural lesions. Histological analysis (H & E staining) revealed a clearly demarked lesion with visible edema and tissue disruption, and the depth of lesion penetration was contingent upon the length of freeze time. For a 60 sec freeze procedure (Fig. 7C), the lesion extended transmurally to the serosa, whereas with a 15 sec freeze, the lesion was localized to the sub-mucosa (Fig. 7D). Analysis of lesion diameter following freezing and 7 day survival revealed, 15 second freeze = 3.9 mm (± 0.2), 30 second freeze = 5.5 mm (± 0.5), 60 second freeze = 7.66 mm (± 2.1) and a 90 second freeze = 12.5 mm (± 2.5 mm) (Table 4). Lesion depth varied based on freeze time and bladder wall thickness which ranged from 3.4 mm to 7.5 mm in the various lesion sites. The 15 sec freezes were found to result in 1.2 (± 0.2) lesion depth with an average wall thickness = 4.8 mm (± 0.1 mm). All of the 30 and 60 second lesions were found to result in the cre-

ation of transmural lesions regardless of bladder wall thickness which ranged from 3 mm to 8 mm (average wall thickness 5.0 mm (± 1.7)). Analysis of the 90 second freeze lesions revealed both sites developed enterovesical fistulas in the bladder wall (average wall thickness 4.5 mm (± 1.6)).

DISCUSSION

The impetus to provide patients and physicians with more advanced, minimally invasive ablative therapies has led to the development of the PSN cryosurgical system. Unlike the majority of commercially available cryoablative devices, which rely on the Joule-Thomson expansion of a gas (eg. Argon), the PSN system uses a mixed phase nitrogen cryogen. Combining liquid and gaseous nitrogen allows for the rapid establishment of the cryogen flow, a traditional hurdle with LN_2 based devices, while at the same time maintaining the ultra-cold nadir temperatures and high thermal conductivity of a liquid cryogen. The ability to rapidly deliver cryogenic temperatures through long lengths of hypodermic tubing allows

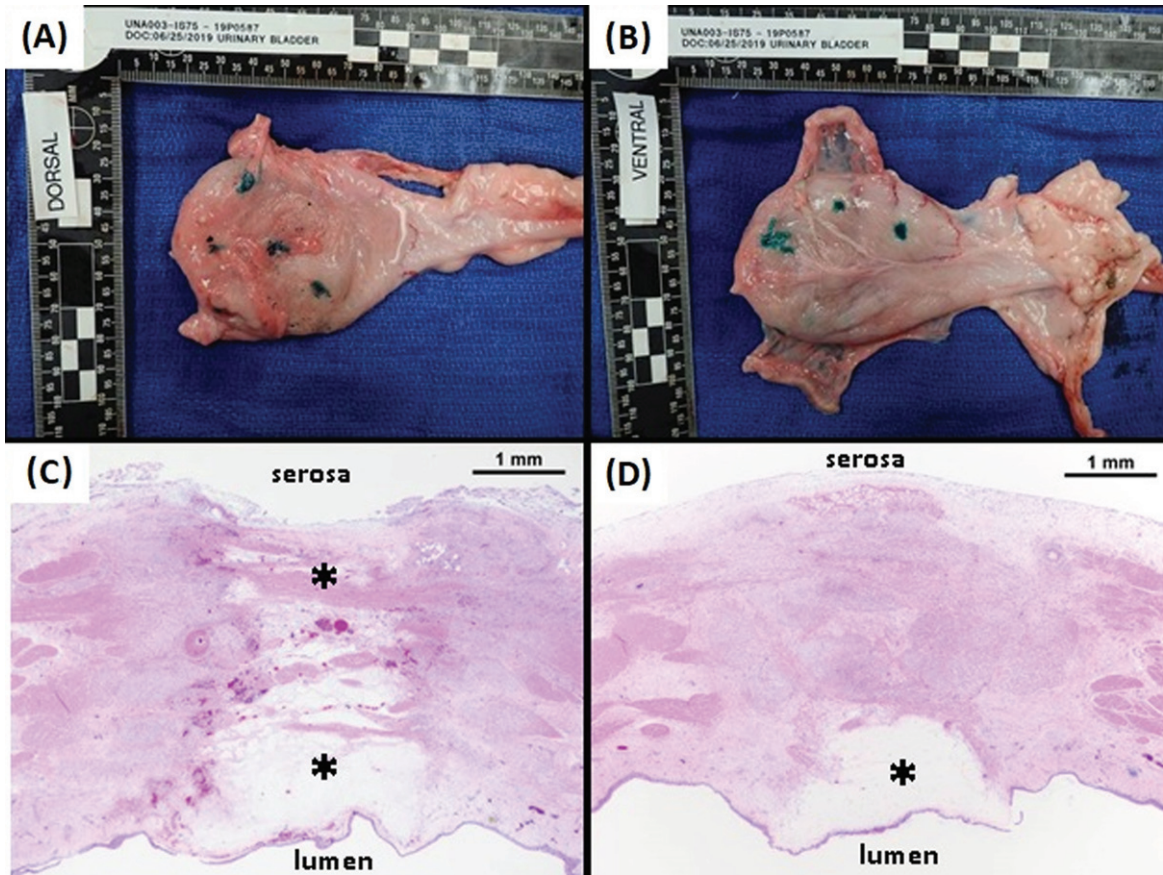


Fig. 7. Gross Pathology and Histology of a Resected Bladder. At 7 days following the *in vivo* procedures bladders were resected and fixed. Gross pathology of the dorsal (A) and ventral (B) serosal surfaces of a bladder revealed numerous transmural lesions (inked sites). Histology (H & E staining) of two representative ablation sites show clearly defined lesions with visible edema and tissue disruption. Lesion depth was contingent on the freeze duration with a 60 sec freeze (C) resulting in ablation of the full thickness of the bladder wall and a 15 sec freeze (D) resulting in an ablative zone confined to the sub-mucosa.

Table 4
Average Lesion Diameter and Depth (\pm SD) in Porcine Bladders 7 Days Post-Freeze

Freeze Time (sec)	Lesion Diameter (mm)	Lesion Depth (mm)	Bladder Wall Thickness (mm)
15 sec	3.9 (0.2)	1.2 (0.2)	4.8 (0.1)
30 sec	5.5 (0.5)	5.2 (1.6)	5.2 (1.6)
60 sec	7.6 (2.1)	4.8 (1.9)	4.8 (1.9)
90 sec	12.5 (2.5)	4.5 (1.6)	4.5 (1.6)

the PSN system to serve as a versatile platform for various cryoprobe configurations. In this study, we evaluated one such cryoprobe, a prototype *FrostBite-BC* cryocatheter, for the transurethral ablation of BCs.

Calorimetric assessment demonstrated that the *FrostBite* cryocatheter yielded an average cooling power of 30.1 W or 0.57 W/mm² of ablation surface area. Cooling power (wattage) is not typically reported for cryoablation probes and is more commonly reported for hyper thermal ablation such as

radio frequency. While not often reported, the limited information available suggests that current argon and nitrous oxide cryoprobes provide in the range of 0.1–0.25 W/mm² of cooling power [18, 44, 48, 49]. As such, the *FrostBite* catheter was found to be significantly more powerful than current cryodevices (2–4 fold increase) [18, 49, 51, 52].

Benchtup assessments of the thermal performance of the cryocatheter using an ultrasound gel revealed a rapid decrease in probe temperatures following probe

activation. Sub-freezing temperatures were observed along the surface of the freeze segment within 6 sec and the critical temperatures of -20°C and -30°C [46] were attained in ≤ 9 sec. Within 15 sec, a catheter tip temperature of $<-85^{\circ}\text{C}$ was achieved and a nadir surface temperature of $<-110^{\circ}\text{C}$ was attained within 30 sec. Assessment of the critical isotherms revealed the penetration of the -20°C isotherm to a depth of 8.5 mm (± 0.8) within 2 mins. This is compared to argon JT based cryosystems where the -20°C isotherm is reported to penetrate <5 mm in 2 mins and ~ 9 mm following 5+ mins of freezing [44, 51, 52]. Depth of penetration of the -20°C and -40°C isotherms are often used as reference points clinically [1, 8, 9, 16, 17, 22, 23]. With the reported minimal lethal temperature for BC in the range of -20°C , we focused on the -20°C isotherm as it represents a potential target isotherm for the treatment of BC [46]. As such, *FrostBite* in conjunction with the PSN system, was found to rapidly deliver the -20°C isotherm deeper than current cryosystems.

Of equal importance to the time to achieve freezing temperatures is the instantaneous cessation of freezing once the ablative procedure has concluded, thereby preventing unintended injury to tissue beyond the targeted area. This can often be an issue with other ablative modalities, such as radio frequency (RF) ablation and radiation, where external energy is applied to the tissue and upon removal of the energy source the large reservoir of energy at the center of the lesion continues to radiate outward [4, 6, 11, 27]. For the treatment of BC, unintended propagation of the ablative lesion could result in damage to the pelvic wall, lower intestines, rectum, the prostate in males, or the uterus and cervix in females. Cryoablation, however, is an energy extractive treatment; once the freeze procedure has concluded, the heat energy from the surrounding tissue begins to flow into the lesion, thus preventing further spread and greatly reducing the possibility of damage to surrounding tissues and organs. With the *FrostBite-BC* cryocatheter, analyses showed that upon stopping the flow of cryogen surface temperatures began to warm near instantaneously (within 1 sec).

Moving beyond freeze performance in ultrasound gel, the *FrostBite-BC* cryocatheter's ablative potential under physiological heat loads was evaluated with an *in vivo*-like, tissue engineered construct. Combining the ability to assess freezing characteristics and cellular responses to cryoablative procedures, the TEM culture model has previously been shown to be a versatile tool in the evaluation of cellular responses

to cryosurgery and cryosurgical technologies for the treatment of prostate [42, 47, 53, 54], kidney [54], and cardiac tissues [44, 48]. Employing the test setup described above, a transurethral cryoablative procedure of BC could be approximated in a laboratory setting with tissue geometries and heat loads analogous to physiological conditions. IR images of the transmural surface of the 3 mm thick TEMs revealed that following a single 2 min freeze procedure the cryocatheter generated a 29.2 mm^2 area below -20°C and a 5.9 mm^2 below -30°C . These areas significantly increased in size to 53.0 mm^2 (an 81.3% increase) and 17.2 mm^2 (an 189.9% increase) respectively following a repeat 2/2/2 min double freeze procedure.

Fluorescent imaging of the TEMs post-thaw revealed ablative diameters that were statistically equivalent for both SCABER and UMUC3-TEM models. Given that *in vitro* models suggest UMUC3 cells are more resistant to freeze injury than SCABER cells (46), these results are encouraging and suggest that the cooling power of the *FrostBite-BC* cryocatheter may overcome minor inherent differences in cell sensitivity. At 24 hr post-thaw, the ablative areas for the SCABER and UMUC3-TEM were found to be between 81.7% and 93.4% of the total frozen volume for both single and repeat 2 min freezes, indicating margins of incomplete cell death of less than 0.6 mm (Figs. 4 & 5). Due to a combination of the recovery following transient cell injury and cellular regrowth in the warmer, non-lethal isotherms of the freeze zone periphery, a reduction in the necrotic zone was observed for both cell types over the course of the recovery period. By 72 hr post-thaw ablative areas had decreased to between 55.0% and 71.0% of the frozen volume (Figs. 4 & 5). Previous studies using the TEM model have shown that this decrease is a result of cellular recovery, infiltration and regrowth in the periphery of the cryogenic lesion where exposure temperatures are non-lethal ($>-10^{\circ}\text{C}$ to 37°C) [42–44, 49]. This phenomenon is typically addressed *in vivo* through the application of a positive freeze margin which ideally ensure that the entirety of the cancerous lesion is contained within the lethal zone of the frozen mass [1, 7, 8]. Nevertheless, despite this *in vitro*-specific recovery, margins of incomplete cell death were still found to be less than 1.6 mm across all conditions at 72 hr post-thaw. Regardless of the recovery, the isotherm and 72 hour viability data obtained with the TEM studies revealed complete cell death in the range of -15°C to -20°C for both SCABER and UMUC3-TEMs following a

single 2 min freeze and from -10°C to -15°C following repeat 2 min freezes using the *FrostBite-BC* cryocatheter. This correlated well with previous *in vitro* reports which suggested that -20°C is the minimal critical temperature for BC cells (SCaBER and UMUC3) [46].

Having established the ability of the *FrostBite-BC* to attain critical temperatures in a rapid and controlled manner, and that by the nature of the cryogen employed with the PSN system (ultra-cold nadir temperatures and high thermal conductivity) critical isotherms can be distributed near the ice-ball periphery, a pilot, *in vivo* porcine study was conducted to evaluate performance. *In vivo* studies revealed freeze times of 15 sec resulted in observable ice on the outer surface of the bladder wall, yet attainment of the -20°C critical isotherm was not achieved transmurally, and thus ablation was confined to the sub-mucosa (Fig. 7D). For freeze times of 30 sec or greater, full thickness ablation was achieved with histological analyses confirming full thickness cell destruction spanning the bladder wall (wall thickness ranged from 3 to 8 mm) (Table 4). Extended freeze times of >90 sec resulted in two lesions developing into enterovesical fistulas. However, in the remaining freeze lesions created using *FrostBite-BC*, eight of which were located adjacent to the bowel, no fistulas were noted regardless of ablation time. It is believed that variability in probe pressure against the bladder wall resulted in increased freezing and lethal temperature penetration at the two fistula sites. One interesting observation was that with the application of a 30 or 60 second freeze, a full thickness transmural ablation was attained across the bladder wall (thickness ranging from 3.2 mm to 8 mm) without any fistula development. While a pilot study, this suggests there may be an application time window which can be applied clinically wherein ablation can be achieved with a reduced risk of development of a fistula. Further studies are needed to fully evaluate this question.

Previous investigations into the use of cryotherapy for the treatment of BCs have primarily employed either argon-JT, percutaneous needles inserted through the abdomen or perineum (36–40), or transurethral cryogen sprays (41). While both approaches have shown promise, both have potential drawbacks and are limited in the types and stages of BCs they can treat. Percutaneous needles are limited to more advanced, muscle invasive cancers (stages 2–4) and the long freeze times (6, 8, or 10 min dual freezes) and tissue penetration may

increase operation costs and the likelihood of infections or other unintended injuries. Cryogen sprays are limited to non-invasive and non-muscle invasive cancers (stages 0–1) and the adiabatic gas expansion may result in fatal pyelovenous gas embolisms and collateral organ injury [41]. Although further investigations are needed into the performance of the *FrostBite-BC* cryocatheter, the results of the pilot *in vivo* study presented here demonstrated a strong correlation between freeze duration and depth of tissue destruction, with short (15 sec) freezes confining the ablative volume to the sub-mucosa (early stage BCs) and longer (≥ 30 sec) freezes ablating the full thickness of the bladder wall (late stage BCs). It may also be possible to control the depth of ablation by controlling the surface temperature of the cryocatheter. It has previously been demonstrated (data not shown) that by modulating the cryogen flow predetermined surface temperatures can be maintained [48, 52]. To this end, our *in vivo* data also supports the notion that the depth of penetration can be controlled through the length of freeze time. This may be important given the variability in bladder wall thickness between patients. Furthermore, as a self-contained, transurethral catheter many of the drawbacks inherent to percutaneous needles and cryogen sprays may be avoided with the *FrostBite-BC* cryocatheter. Another observation from this pilot study was the ability to create multiple lesions within a subject's bladder during a procedure without issue. This suggests that multi-focal tumors may be targeted with the application of multiple freezes. While promising, this *in vivo* study has several limitations. Firstly, the pilot study was limited to 24 lesions in two subjects. Secondly, the study was conducted in healthy bladders. Lastly, analysis was limited to H & E staining following 7 days survival. Future studies will focus on an expanded cohort, inclusion of trichrome staining to examine extent of cell death within a lesion to confirm transmural destruction, *in vivo* tumor models, as well as correlation of application time and temperatures with lesion depths in an effort to develop procedural "dosing" parameters yielding tumor destruction while reducing/eliminating the threat of over-freezing, fistula development and damaging non-targeted tissues and organs.

CONCLUSIONS

With the recent success and growth of cryoablation there is now a movement toward its increased

utilization as well as desire for improved procedural outcomes. In order to achieve this in an effective, time efficient manner, new cryotechnologies are being developed to facilitate rapid tissue cooling to more effectively ablate tissue. This study investigated the performance of one such system, the PSN cryoconsole, in combination with a novel cystoscopic compatible cryoablation catheter for targeted ablation of BC. We hypothesized that through the use of *FrostBite-BC*, rapid, effective, minimally invasive ablation of bladder tissue could be achieved. Through a combination of *in vitro* and *in vivo* evaluations, it was determined that the *FrostBite-BC* cryocatheter possesses the ability to deliver rapid, effective ablative doses in a controlled and predictable manner. The data presented herein demonstrate that *FrostBite-BC* provided for the rapid and effective delivery of a cryoablative “thermal dose” (-20°C) deep into a frozen tissue mass within 60 seconds under physiological conditions (37°C). The results further support the potential for targeting multi-focal disease with the application of multiple freeze sites during a procedure. While the results of this study are promising, given their investigational nature the extent of conclusions which can be drawn are limited; however, the data does suggest that this technology holds promise and that continued assessment of the technology *in vivo* is warranted. Overall, this study suggests that the *FrostBite-BC* cryocatheter may offer promise as a next generation cryoablation device allowing for the rapid and controlled application of ultra-cold temperatures and efficient freezing of targeted tissue for the treatment of BCs.

ACKNOWLEDGMENTS

The authors would like to thank Ms. Courtney McLaughlin and Ms. Gabrielle String, MS for their contributions to data acquisition for this manuscript. The authors would also like to acknowledge and thank Ms. Janelle Schmidt (APS Study Business Development Associate), Ms. Liisa Carter (APS Study Director) and Mr. Tyler LaMont (APS Study Interventionalist) and the entire APS staff for their diligence and assistance in executing the *in vivo* studies.

FUNDING

This study was supported in part by funding from the National Institutes of Health National Cancer

Institute Grant No. 1R43CA210761-01A1 awarded to CPSI Biotech.

CONFLICTS OF INTEREST

Financial: ATR, JMB, KLS, KKS and RVB are employees of CPSI Biotech. *Non-Financial:* JGB, AK and AC served in an advisory role to CPSI as collaborators on this project. JMB and JGB are related.

AUTHOR CONTRIBUTIONS

Conception: ATR, JMB, KLS and KKS performed study design. RVB, JGB, AC, AK provided review and feedback on study design.

Performance of Work: ATR, JMB, KLS and KKS performed all experimental designs and experimentation for this study.

Interpretation or Analysis of Data: JMB, ATR, KKS and KLS conducted data analysis and interpretation. AK, AC, RVB and JGB reviewed and provided guidance and feedback on data analysis and interpretation.

Writing the Article: JMB and ATR prepared the draft manuscript. JMB prepared the revised manuscript. ATR, KLS, KKS, RVB, AK, AC and JGB provided revision input for the manuscript. All authors read and approved the final manuscript.

AVAILABILITY OF DATA AND MATERIAL

The data that support the findings of this study are available from CPSI Biotech but restrictions apply to the availability of these data, which were used under license for the current study, and so are not publicly available. Data are however available from the authors upon reasonable request and with permission of CPSI Biotech.

REFERENCES

- [1] Babaian RJ, Donnelly B, Bahn D, Baust JG, Dineen M, Ellis D, et al. Best practice statement on cryosurgery for the treatment of localized prostate cancer. *J Urol*. 2008;180(5):1993-2004.
- [2] Baust JG, Gage AA, Robilotto AT, Baust JM. The pathophysiology of thermoablation: optimizing cryoablation. *Curr Opin Urol*. 2009;19(2):127-32.
- [3] Gage AA, Baust JM, Baust JG. Experimental cryosurgery investigations *in vivo*. *Cryobiology*. 2009;59(3):229-43.
- [4] Kuhne M, Suter Y, Altmann D, Ammann P, Schaer B, Osswald S, et al. Cryoballoon versus radiofrequency catheter ablation of paroxysmal atrial fibrillation: biomarkers of myocardial injury, recurrence rates, and pulmonary vein

- reconnection patterns. *Heart Rhythm*. 2010;7(12):1770-6.
- [5] Kojodjojo P, O'Neill MD, Lim PB, Malcolm-Lawes L, Whinnett ZI, Salukhe TV, et al. Pulmonary venous isolation by antral ablation with a large cryoballoon for treatment of paroxysmal and persistent atrial fibrillation: medium-term outcomes and non-randomised comparison with pulmonary venous isolation by radiofrequency ablation. *Heart*. 2010;96(17):1379-84.
- [6] Chan NY, Choy CC, Lau CL, Lo YK, Chu PS, Yuen HC, et al. Cryoablation versus radiofrequency ablation for atrioventricular nodal reentrant tachycardia: patient pain perception and operator stress. *Pacing Clin Electrophysiol*. 2011;34(1):2-7.
- [7] Correas JM, Delavaud C, Gregory J, Le Guilchet T, Lamhaut L, Timsit MO, et al. Ablative Therapies for Renal Tumors: Patient Selection, Treatment Planning, and Follow-Up. *Semin Ultrasound CT MR*. 2017;38(1):78-95.
- [8] Gage AA, Baust JG. Cryosurgery for tumors - a clinical overview. *Technol Cancer Res Treat*. 2004;3(2):187-99.
- [9] Cohen JK, Miller RJ, Ahmed S, Lotz MJ, Baust J. Ten-year biochemical disease control for patients with prostate cancer treated with cryosurgery as primary therapy. *Urology*. 2008;71(3):515-8.
- [10] Defaye P, Kane A, Jacon P, Mondesert B. Cryoballoon for pulmonary vein isolation: Is it better tolerated than radiofrequency? Retrospective study comparing the use of analgesia and sedation in both ablation techniques. *Arch Cardiovasc Dis*. 2010;103(6-7):388-93.
- [11] Liu E, Shehata M, Liu T, Amorn A, Cingolani E, Kannarkat V, et al. Prevention of esophageal thermal injury during radiofrequency ablation for atrial fibrillation. *J Interv Card Electrophysiol*. 2012;35(1):35-44.
- [12] Snyder KK, Baust J.G., Baust J.M., Gage A.A. Mechanisms of Cryoablation. In: Bredikis AJ WD, editor. *Cryoablation of Cardiac Arrhythmias*. St Louis: W.B. Saunders; 2011. p. 13-21.
- [13] Gage AA, Snyder KK, Baust JM, Baust JG. The Principles of Cryobiology. In: Dubac M KP, editor. *Cryoablation for Cardiac Arrhythmias*. Quebec, Canada: Vision Commun.; 2008. p. 3-12.
- [14] Canto MI, Dunbar, K., Wang, J., Montgomery, E., Okolo, P. Low Flow CO₂-cryotherapy for primary and "rescue" endoscopic therapy of Barrett's esophagus with high grade dysplasia or early adenocarcinoma. [Poster] 2008. Available from: <http://www.gi-supply.com/wp-content/uploads/2014/06/canto-cryo-poster.pdf>.
- [15] Baust JG, Snyder KK, Santucci KL, Robilotto AT, Van Buskirk RG, and Baust JM. Cryoablation: physical and molecular basis with putative immunological consequences. *Int J Hyperthermia*. 2019;36(sup1):10-6.
- [16] Baust JM, Rabin Y, Polascik TJ, Santucci KL, Snyder KK, Buskirk RG, et al. Defeating Cancer's Adaptive Defensive Strategies Using Thermal Therapies: Examining Cancer's Therapeutic Resistance, Ablative, and Computational Modeling Strategies as a means for Improving Therapeutic Outcome. *Technology in Cancer Research & Treatment*. 2018;17:1533033818762207.
- [17] Abdo J, Cornell DL, Mittal SK, Agrawal DK. Immunotherapy Plus Cryotherapy: Potential Augmented Abscopal Effect for Advanced Cancers. *Front Oncol*. 2018; 8:85.
- [18] Baust JM, Robilotto AT, Gage AA, Baust JG. Enhanced Cryoablative Methodologies. In: Bischof JCaX, Y., editor. *Multiscale Technologies for Cryomedicine*: World Scientific Publishing Co; 2016. p. 388.
- [19] Gessl I, Waldmann E, Penz D, Majcher B, Dokladanska A, Hinterberger A, et al. Resection rates and safety profile of cold vs. hot snare polypectomy in polyps sized 5-10mm and 11-20mm. *Dig Liver Dis*. 2019;51(4):536-41.
- [20] Li Z, Fu Y, Li Q, Yan F, Zhao J, Dong X, et al. Cryoablation plus chemotherapy in colorectal cancer patients with liver metastases. *Tumour Biol*. 2014;35(11):10841-8.
- [21] Scholvinck DW, Kunzli HT, Kestens C, Siersema PD, Vlegaar FP, Canto MI, et al. Treatment of Barrett's esophagus with a novel focal cryoablation device: a safety and feasibility study. *Endoscopy*. 2015;47(12):1106-12.
- [22] Polascik TJ, Mayes JM, Mouraviev V. Nerve-sparing focal cryoablation of prostate cancer. *Curr Opin Urol*. 2009;19(2):182-7.
- [23] Sabel MS. Cryoablation for breast cancer: no need to turn a cold shoulder. *J Surg Oncol*. 2008;97(6):485-6.
- [24] Callstrom MR, Dupuy DE, Solomon SB, Beres RA, Littrup PJ, Davis KW, et al. Percutaneous image-guided cryoablation of painful metastases involving bone: multicenter trial. *Cancer*. 2013;119(5):1033-41.
- [25] Ba YF, Li XD, Zhang X, Ning ZH, Zhang H, Liu YN, et al. Comparison of the analgesic effects of cryoanalgesia vs. parecoxib for lung cancer patients after lobectomy. *Surg Today*. 2015;45(10):1250-4.
- [26] Cox JL, Boineau JP, Schuessler RB, Jaquiss RD, Lappas DG. Modification of the maze procedure for atrial flutter and atrial fibrillation. I. Rationale and surgical results. *J Thorac Cardiovasc Surg*. 1995;110(2):473-84.
- [27] Schwagten B, Knops P, Janse P, Kimman G, Van Belle Y, Szili-Torok T, et al. Long-term follow-up after catheter ablation for atrioventricular nodal reentrant tachycardia: a comparison of cryothermal and radiofrequency energy in a large series of patients. *J Interv Card Electrophysiol*. 2011;30(1):55-61.
- [28] Yorgun H, Canpolat U, Oksul M, Sener YZ, Ates AH, Crijns H, et al. Long-term outcomes of cryoballoon-based left atrial appendage isolation in addition to pulmonary vein isolation in persistent atrial fibrillation. *Europace*. 2019;21(11):1653-62.
- [29] Friedman PL. Catheter cryoablation of cardiac arrhythmias. *Curr Opin Cardiol*. 2005;20(1):48-54.
- [30] Cronin KA, Lake AJ, Scott S, Sherman RL, Noone AM, Howlader N, et al. Annual Report to the Nation on the Status of Cancer, part I: National cancer statistics. *Cancer*. 2018;124(13):2785-800.
- [31] Sievert KD, Amend B, Nagele U, Schilling D, Bedke J, Horstmann M, et al. Economic aspects of bladder cancer: what are the benefits and costs? *World J Urol*. 2009;27(3):295-300.
- [32] Goikhsberg MI, Zaporin VK, Klimenko IA, Kinevskii OF. Cryosurgical treatment of bladder cancer. *Urol Nefrol (Mosk)*. 1979;(2):24-7.
- [33] Reuter HJ. Endoscopic cryosurgery of prostate and bladder tumors. *J Urol*. 1972;107(3):389-93.
- [34] Rigondet G. Cryotherapy in bladder tumours. *Prog Clin Biol Res*. 1984;162B:355-8.
- [35] Liu S, Zou L, Mao S, Zhang L, Xu H, Yang T, et al. The safety and efficacy of bladder cryoablation in a beagle model by using a novel balloon cryoprobe. *Cryobiology*. 2016;72(2):157-60.
- [36] Liu S, Zhang L, Zou L, Wen H, Ding Q, Jiang H. The feasibility and safety of cryoablation as an adjuvant therapy with transurethral resection of bladder tumor: A pilot study. *Cryobiology*. 2016;73(2):257-60.

- [37] Zhang Q, Zhang S, Wang W, Zhao X, Deng Y, Lian H, et al. Transperineal cryotherapy for unresectable muscle invasive bladder cancer: preliminary experience with 7 male patients. *BMC Urol.* 2017;17(1):81.
- [38] Permpongkosol S, Nicol TL, Kavoussi LR, Jarrett TW. Percutaneous bladder cryoablation in porcine model. *J Endourol.* 2006;20(12):991-5.
- [39] Liang Z, Fei Y, Lizhi N, Jianying Z, Zhikai Z, Jibing C, et al. Percutaneous cryotherapy for metastatic bladder cancer: experience with 23 patients. *Cryobiology.* 2014;68(1):79-83.
- [40] Sun L, Zhang W, Liu H, Yuan J, Liu W, Yang Y. Computed tomography imaging-guided percutaneous argon-helium cryoablation of muscle-invasive bladder cancer: initial experience in 32 patients. *Cryobiology.* 2014;69(2):318-22.
- [41] Power NE, Silberstein JL, Tarin T, Au J, Thorner D, Ezell P, et al. Endoscopic spray cryotherapy for genitourinary malignancies: safety and efficacy in a porcine model. *Ther Adv Urol.* 2013;5(3):135-41.
- [42] Robilotto AT, Baust JM, Van Buskirk RG, Gage AA, Baust JG. Temperature-dependent activation of differential apoptotic pathways during cryoablation in a human prostate cancer model. *Prostate Cancer Prostatic Dis.* 2013;16(1):41-9.
- [43] Robilotto AT, Clarke D, Baust JM, Van Buskirk RG, Gage AA, Baust JG. Development of a tissue engineered human prostate tumor equivalent for use in the evaluation of cryoablative techniques. *Technol Cancer Res Treat.* 2007;6(2):81-9.
- [44] Baust JM, Robilotto A, Snyder KK, Santucci K, Stewart J, Van Buskirk R, et al. Assessment of Cryosurgical Device Performance Using a 3D Tissue-Engineered Cancer Model. *Technol Cancer Res Treat.* 2017 Jan 01.
- [45] Baust JG, Smith JT, Santucci KL., Snyder KK, Robilotto AT, Van Buskirk RG, Baust JM, Corwin WL, McKain JF. inventor Tissue Engineered Model and Method of Use patent 9,213,025. 2015.
- [46] Santucci KL, Baust JM, Snyder KK, Van Buskirk RG, Katz, A., Corcoran, A., Baust JG. Investigation of Bladder Cancer Cell Response to Cryoablation and Adjunctive Cisplatin Based Cryo/Chemotherapy. *Clin Res Open Access.* [Journal]. 2020 07 February 2020;6(1).
- [47] Klossner DP, Robilotto AT, Clarke DM, VanBuskirk RG, Baust JM, Gage AA, et al. Cryosurgical technique: assessment of the fundamental variables using human prostate cancer model systems. *Cryobiology.* 2007;55(3):189-99.
- [48] Baust JM, Robilotto A, Guerra P, Snyder KK, Van Buskirk RG, Dubuc M, et al. Assessment of a novel cryoablation device for the endovascular treatment of cardiac tachyarrhythmias. *SAGE Open Med.* 2018;6: 2050312118769797.
- [49] Robilotto AT, Baust JM, Santucci KL, Snyder KK, Van Buskirk RG. Assessment of a novel supercritical nitrogen cryosurgical device using prostate and renal cancer tissue engineered models. *Medical Devices and Diagnostic Engineering.* 2019;5:1-8.
- [50] Baust JM, Robilotto AT, Snyder KK, Santucci KL, Stewart JF. Assessment of cryosurgical device performance using an *in vivo* like 3D tissue engineered cancer model. *Technol Cancer Res Treat.* 2017;16(6):900-9.
- [51] Littrup PJ, Jallad B, Vorugu V, Littrup G, Currier B, George M, et al. Lethal isotherms of cryoablation in a phantom study: effects of heat load, probe size, and number. *J Vasc Interv Radiol.* 2009;20(10):1343-51.
- [52] Shah TT, Arbel U, Foss S, Zachman A, Rodney S, Ahmed HU, et al. Modeling Cryotherapy Ice Ball Dimensions and Isotherms in a Novel Gel-based Model to Determine Optimal Cryo-needle Configurations and Settings for Potential Use in Clinical Practice. *Urology.* 2016;91:234-40.
- [53] Clarke DM, Robilotto AT, Van Buskirk RG, Baust JG, Gage AA, Baust JM. Targeted induction of apoptosis via TRAIL and cryoablation: a novel strategy for the treatment of prostate cancer. *Prostate cancer and prostatic diseases.* 2007;10(2):175-84.
- [54] Clarke DM, Robilotto AT, Rhee E, VanBuskirk RG, Baust JG, Gage AA, et al. Cryoablation of renal cancer: variables involved in freezing-induced cell death. *Technol Cancer Res Treat.* 2007;6(2):69-79.